



Efficient inverted all inorganic CsPbI₃ planar solar cells via twice-coating in air condition

Aziz Saparbaev^{a,c}, Chenglin Gao^{a,b}, Dangqiang Zhu^a, Zhilin Liu^{a,b}, Xiaofei Qu^b, Xichang Bao^{a,*}, Renqiang Yang^{a,**}

^a CAS Key Laboratory of Bio-based Materials, Qingdao Institute of Bioenergy and Bioprocess Technology, Chinese Academy of Sciences, Qingdao, 266101, China

^b College of Materials Science and Engineering, Qingdao University of Science and Technology, Qingdao, 266042, PR China

^c Center of Materials Science and Optoelectronics Engineering, University of Chinese Academy of Sciences, Beijing, 100049, China

HIGHLIGHTS

- High quality CsPbI₃ films was prepared via twice-coating technique.
- The pinholes and trap density of the films during quickly second drip coating.
- Power conversion efficiency of 11.05% was obtained in inverted planar PSCs.

ARTICLE INFO

Keywords:

Perovskite solar cells
Cesium lead triiodide
Twice coating technique
High performance
Charge recombination

ABSTRACT

Recently, solar cells based on inorganic cesium lead triiodide perovskite materials have received considerable attention. However, the quality and thickness of perovskite films are still out from satisfaction due to the limited solubility of the precursor materials. Here, a simple twice-coating process is reported for fabrication of high-quality perovskite films in a complete air condition. Defects such as pinholes, can be effectively eliminated by the second coating with further growth of the grain sizes, thus greatly suppressing charge recombination in these perovskite films. Furthermore, the improved film thickness can ameliorate the absorption of incident light. In consequence, the power conversion efficiency of 11.05% with comprehensively improved device parameters is obtained in traditional inverted planar perovskite solar cells, with a dramatic increase of 42% being compared with the control device (7.83%). In addition, the device's stability is also improved due to such high quality twice-coated perovskite films. The results reveal that such twice-coating technique is a promising choice for high-stabilty and efficient perovskite solar cells.

1. Introduction

Within the last decade, photovoltaic devices for both organic solar cells (OSCs) and perovskite solar cells (PSCs) have received considerable attention as new generation renewable energy sources based on such advantageous features as low cost, flexibility, light weight, and both environmental- and economical-friendly solution-processed fabrication [1–6]. For the latter, perovskite materials have been focused extensively due to its excellent photophysical properties and other wide applications [7–10]. Great efforts have been expended to develop high performance PSCs, and power conversion efficiency (PCE) from 3.8% for the first time in 2009 [11] was rapidly boosted to over 23% just within few years [12–14], making PSCs the fastest advancing

photovoltaic technology to date. However, the life time of these solar cells turns to be crucial for practical applications. Even though great improvements have been recently achieved for organic–inorganic PSCs with improved quality of the active layers and high stable interface materials, the perovskite layer still slowly decomposes into lead iodide and organic component due to such defects of organic component (MA, FA) as their easy sublimation, moisture corrosion, and photo oxidation [15–18]. One method for keeping from these problems is to replace the organic part with an inorganic element to obtain all inorganic PSCs, and recent results have pronounced good photostability, humidity and thermal stability on such devices.

Among all-inorganic metal halide perovskites, CsPbI₃ with the cubic phase (α -CsPbI₃) possesses suitable bandgap (~ 1.7 eV) for photovoltaic

* Corresponding author.

** Corresponding author.

E-mail addresses: baoxc@qibebt.ac.cn (X. Bao), yangrq@qibebt.ac.cn (R. Yang).

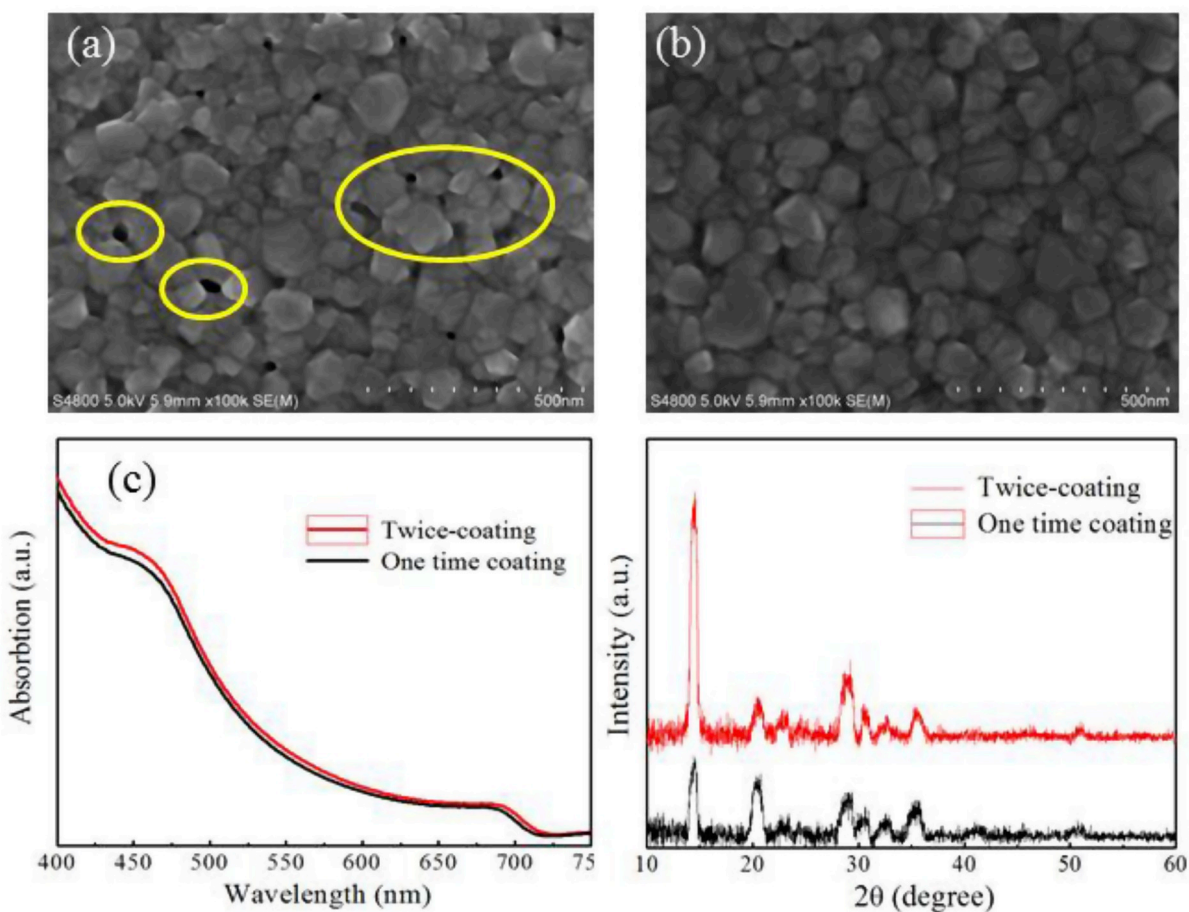


Fig. 1. SEM images (a, b), absorption spectra (c), and XRD patterns (d) of the perovskite films under different conditions.

applications [19–21]. However, the desired α -CsPbI₃ material could usually be formed at high temperature of above 310 °C via traditional methods leading to rapid degradation to the undesired δ -phase under atmosphere at room temperature, which have large bandgap (~2.8 eV) being unsuitable for photovoltaic applications [22,23]. In addition, the thickness of the photoactive layer prepared under traditional conditions is limited due to the poor solubility of precursor materials, which restricts the light utilization. Furthermore, the as-prepared films have many defects, such as pinholes and cracks, which results in poor device performance [24,25]. In 2016, Luo et al. introduced hydroiodic acid (HI) as an additive into the precursor and further used isopropanol for post treatment for fabricating efficient CsPbI₃ PSCs, resulting in stable α -CsPbI₃ at low-temperature phase-transition route [26]. Since then, several efforts for further improving the quality of photoactive films have been adapted, such as introducing small amount of additives into the perovskite precursors [27,28], post surface treatment to further improve the crystal grain growth and/or enhance the phase stability [29–31], and developing new growth methods for high quality and stable α -CsPbI₃ film [32,33]. For practical applications, simple and low-cost fabrication processes with thick high-quality active layers are still highly desirable for further development of these inorganic solar cells.

In this work, a simple twice-coating process for fabrication high-quality perovskite films in full air conditions is reported. After firstly preparing one layer of perovskite, we quickly drip-coated once more on the top of them. Through this method, the thickness of the prepared perovskite layer is obviously increased, and the defects such as pinholes and cracks in the film can be effectively eliminated, thus resulting in a PCE of 11.05% with an improvement of 41% compared to the control device (7.83%) in the inverted planar devices.

2. Experimental section

2.1. Materials

Cesium Iodine (CsI) and Lead Iodine (PbI₂) were bought from Xi'an Polymer Light Technology Inc (China). The poly(3,4-ethylenedioxythiophene)/poly(styrenesulfonate) (PEDOT:PSS) aqueous solution (Clevios PVP Al4083) and [6,6]-phenyl-C61-butyric acid methyl ester (PC₆₁BM) were purchased from H. C. Starck (Leverkusen, Germany) and American Dye Sources Inc. (Baie-d'Urfe, Quebec, Canada), respectively. Lithium fluoride (LiF, 99.99%) and hydroiodic acid (HI, 45 wt%) were obtained from Sinopharm Chemical Reagent Co., Ltd. (Shanghai, China). The above materials were used as received. Indium tin oxide (ITO) coated glass substrates with a sheet resistance of 15 Ω sq⁻¹ were provided by Shenzhen Display (Shenzhen, China).

2.2. Device fabrication and characterizations

ITO-coated glass substrates were cleaned by ultrasonication in acetone, deionized (DI) water and isopropyl alcohol (IPA) for 13 min each and then dried using high purity nitrogen gas. The substrates were then treated with oxygen plasma for 6 min. Afterwards, 40 nm PEDOT:PSS was spin-coated (4000 rpm, 20 s) on the substrates, and then baked in an oven at 160 °C for 20 min under air conditions. To form the CsPbI₃ precursor solution, CsI and PbI₂ were dissolved in DMF with 1:1 M ratio (0.5 M) and stirred for 24 h in air. 66 μ L of HI acid was added into 1 mL precursor solution before prepare perovskite films. Then, the perovskite films were prepared by spin-coating the precursor solution on the substrates at 4000 rpm for 10 s. In order to improve the

film quality and film thicknesses, quickly drip coating process was repeated once more. The substrates were subsequently heated at 100 °C for 10 min on a hot plate under air conditions (Fig. S1a). The color of the films changed from transparent light yellow to dark brown. After that, 50 nm PC₆₁BM was spin-coated (1500 rpm, 20 s) on the CsPbI₃ films. The cathode consisting LiF (1 nm) and Al (100 nm) was deposited at a base pressure of 5×10^{-4} Pa using a thermal evaporator. The device structure is illustrated in Fig. S1b and the active area of the devices is 0.1 cm² defined by a shadow mask.

The absorption spectra of the films on ITO glass were obtained on a scanning spectrophotometer (Varian Cary 50 UV/vis, Palo Alto, CA). Bruker D8 ADVANCE was applied to record the X-ray diffraction (XRD) patterns for perovskite films. Surface morphology of the films were characterized by Hitachi S-4800 scanning electron microscopy (SEM). The thicknesses of the films were measured by Veeco Dektak 150 surface profiler. The current density–voltage (J – V) characteristics were recorded with a Keithley 2420 source measurement unit under simulated 100 mW cm⁻² (AM 1.5 G) irradiation from a Newport solar simulator. The photoluminescence spectra were obtained on a Horiba Jobin Yvon FluoroMax-4 Bench-top Spectrofluorometer.

3. Results and discussion

Commonly, the α -CsPbI₃ perovskite layers are usually prepared from the precursor solution of CsI and PbI₂ with proper HI additive so that they can crystallize at low processed temperature of about 100 °C [24]. The image of as-prepared layers presented very smooth surface as shown in Fig. S2a. However, from the SEM images of Fig. 1a and the Figs. S3a and c, there found a great number of pinholes which were consistent with previously reported results [24,25]. This would result in lots of defects, and/or trap density as recombination centers, and reduce shunt resistance leading to poor device performance [34]. After quickly drip-coating it once more, the holes had been well repaired as shown in Fig. 1b and Figs. S3b and c. Furthermore, it was found that the grain size of the perovskite crystal had been grown further. Fig. 2c shows the UV–Vis absorption spectra of the perovskite layers under two conditions. These two films reveal similar curvature with absorption a wide range of light, indicating the formation of α -CsPbI₃ perovskite. Interestingly, the film's absorption intensity has been obviously enhanced by second coating, especially at short wavelength region. It can be shown that the pinholes are fixed and the thickness was increased (from 212 nm for one time to 251 nm for twice-coating sample) for the films with twice-coating method. In addition, XRD was carried out to characterize the crystal structures of the perovskite films prepared under different conditions, as shown in Fig. 1d. One can see that there have found (100), (110), (200), (211), and (220) diffraction peaks in both films proving the formation of cubic crystal phase of CsPbI₃ [35–37]. In terms of peak intensity, the films forms with second coating were significantly enhanced, as a sign of crystal re-growth, which is agreed by the results from SEM results. The average grain size calculated by the Scherrer formula is about 43 nm and 55 nm for one time coating and twice-coating sample along the (110) peak, respectively [38–40]. It can be speculated that the improved grain size and film thickness combined with repaired surface morphologies has led to the increased device performance, and will be further discussed below.

Hence, inverted planar heterojunction perovskite solar cells with a structure of ITO/PEDOT:PSS/perovskite film/PC₆₁BM/LiF/Al were fabricated in full air conditions. As a reference, the control device with the perovskite layer coated only once was also prepared. Fig. 2a and Table 1 shows current density–voltage (J – V) curves and their relevant device parameters. The control device exhibits a PCE of 7.83% under reversed scans with a short-circuit current density (J_{SC}) of 12.24 mA cm⁻², an open circuit voltage (V_{OC}) of 0.94 V, and a fill factor (FF) of 68.07% under AM 1.5 G illumination, which is comparable to

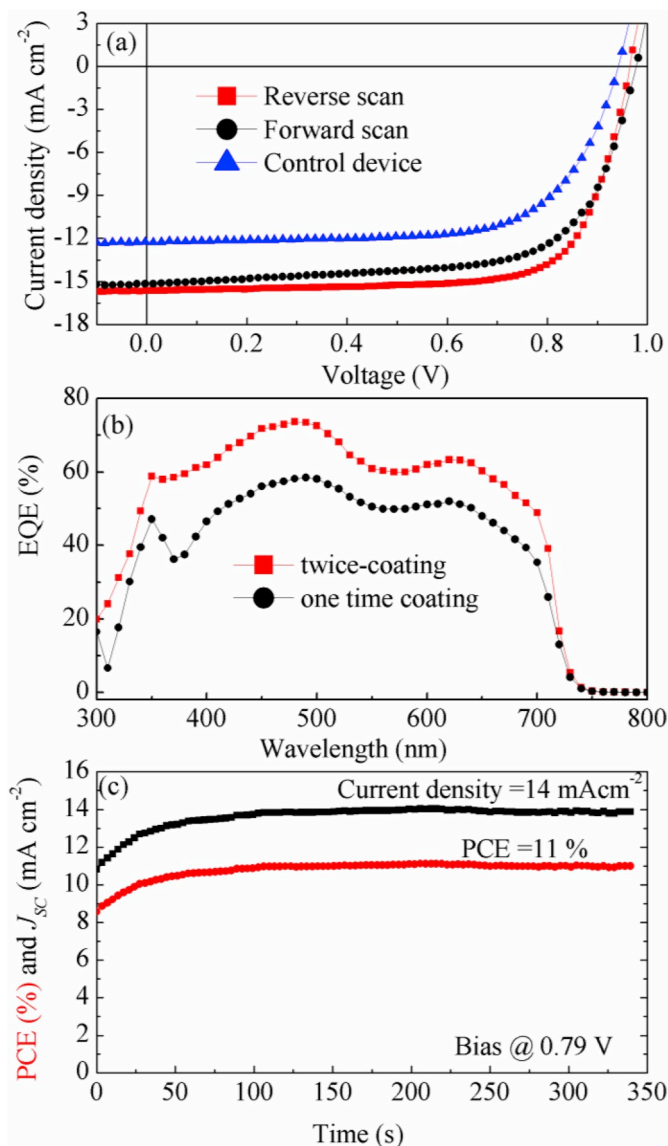


Fig. 2. J – V curves (a), EQE spectra (b) of the photovoltaic devices, and the stable power output of the optimized device.

$$V_{OC} = \frac{kT}{q} \ln \frac{J_s}{J_0} + 1$$

Table 1

Device parameters of the solar cells under different prepare conditions.

device	V_{OC} (V)	J_{SC} (mA cm ⁻²)	FF (%)	PCE (%)	R_{series} (Ω)
Reverse scan	0.97	15.65	73.14	11.05	4.87
Forward scan	0.98	15.54	65.69	9.99	7.02
Control device	0.94	12.24	68.07	7.83	6.52

the previous reports using the similar method [26]. However, its photovoltaic performance was still limited by the relatively low J_{SC} , V_{OC} , and FF. As above discussed, one reason is that such one spin-coated the perovskite films possessed lots of pinholes and the grain sizes of the control films were relative small which would result in the serious charge recombination, and thus poor J_{SC} . Another reason is the limited thickness of the perovskite films prepared under traditional conditions due to the poor solubility of precursor materials, which refined their

light utilization. If the film thickness is increased by lowering the coating speed, the device performance becomes worse (Fig. S4). After modification with fast drip-coating once more with the perovskite precursors, the film thickness and surface morphology of the films had been greatly improved with almost fully eliminated pinholes and re-grown grain sizes. These results imply that twice-coating process could effectively eliminate the defect and trap density in the perovskite film and thus improve the charge transport. Hence, the PCE of the device reached up to 11.05% with a small hysteresis, and all related device parameters including J_{SC} (15.65 mA cm^{-2}), V_{OC} (0.97 V), and FF (73.14%) have been effectively improved. It is known that there have a photo current dependency on V_{OC} , i.e., where J_s is the photocurrent density, J_0 is the saturation current density, k is the Boltzmann constant, T stands for temperature, and q represents the Coulomb charge. As discussed above, the J_{SC} can be effectively improved from 12.24 to 15.65 mA cm^{-2} after spin coating once more. The V_{OC} has a similar trend according to the equation, further confirming the validity of the treatment.

The defects and thickness of the modified perovskite film can be effectively improved, which will homogeneously enhance the photo-response in the whole range. The EQE spectra of the devices are given in Fig. 2b, and they are closely consistent with the absorption spectra of the perovskite. Furthermore, although similar shape for the devices without or with second coating are pronounced, the EQE values for the device with second coating are higher than those of only once coated device, which is in line with the results from J - V curves. In addition, the power output over time at a fixed voltage under maximum power point (0.79 V) on the J - V curve was also measured, as shown in Fig. 2c. A high stable output with a PCE of 11.0% and a J_{SC} of 14.1 mA cm^{-2} was obtained for the device with second coating, keeping almost constant in long time scale. Such high and stable power output efficiency could be attributed to the improved quality of the perovskite layer with quickly second coating. Furthermore, device stability of PSCs with second coating was also tested in glove box, and the results are given in Table S1. After 60 days, the device still claimed a PCE of 7.50%, indicating such twice-coating technique is an effective method for improving both efficiency and stability.

It is known that the defect and/or trap density in the photoactive layers can act as charge recombination centers, which can significantly affect device performance [41]. In order to further investigate the effect of film quality on improvements of device performance, PL spectra were collected for the perovskite films on quartz glass, which can avoid the influence of charge injection between the perovskite and the electrode [42,43]. As can be seen in Fig. 3a, the intensity of the perovskite film with only one-time coating appears very weak and that of the secondly coated films increases greatly. The enhanced PL intensity indicates that both the defect and trap density has been effectively suppressed in the secondly coated films. From the aspect of device performance, the photocurrent (such as J_{SC}) versus different light intensity (P) can give a more in-depth insight into the charge recombination characteristics, and can be used as a method to distinguish the quality of the films. Generally, there is a power-law dependency of the incident light intensity (P) on the photocurrent (J_{SC}), i.e. $J_{SC} \propto P^S$, where S is a power index [44,45]. The closer the S value is to 1, the less charge recombination and the more freely charge transport would happen and thus better film quality there obtained. As can be seen in Fig. 3b, the fitting value of S for device based on the secondly coated film is 0.981, being a bit higher than that for the one based on one-time coating (0.972), which is much closer to 1. These results further demonstrate that twice-coating technique can effectively improve the film quality and device performance.

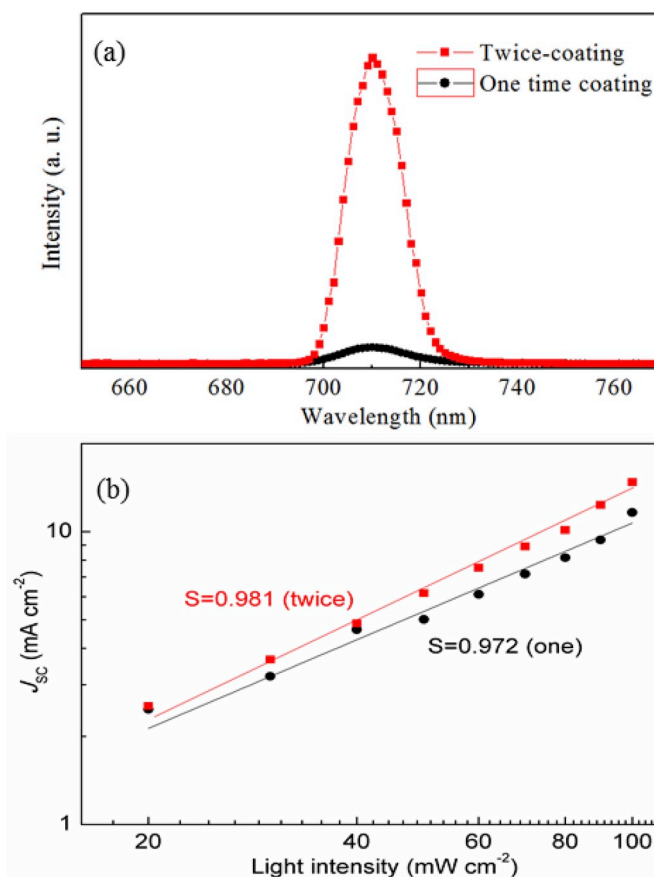


Fig. 3. PL spectra the perovskite films on the glass substrate (a) and J_{SC} versus light intensity of the devices (b) under different conditions.

For concluding whether or not the method is effective, the reproducibility of photovoltaic performance of the solar cells is of great importance. Herein 44 separate devices were fabricated and tested using the previous second-coating technique. Fig. 4 shows the histograms of the device-performance parameters. As illustrated in Fig. 4, the J_{SC} , V_{OC} , and FF of all devices have been greatly improved compared to the control device, thus leading to an average PCE of 9.92%. It is known that the film quality of perovskite is a key factor for the fabrication of efficient PSCs. The pinholes in the perovskite films were effectively eliminated and the grain sizes re-grow once more via such quickly second-coating technique. Meanwhile the film thickness was improved. In short, the high performance for all devices is due to their greatly improved quality of the photoactive layers.

4. Conclusion

In summary, high quality perovskite films were obtained by twice-coating technique under atmospheric conditions. The results demonstrate that pinholes of the films can be effectively eliminated and the grain sizes re-grow once more and their charge recombinations can be greatly inhibited as well. Furthermore, the film thickness has been improved to make better use of incident light intensity. Consequently, efficient inverted all inorganic α -CsPbI₃ PSCs exhibits high PCE of 11.05% with all improved device parameters. The findings in this work show that simple methods can effectively improve device performance, and pave a way for potential practical applications.

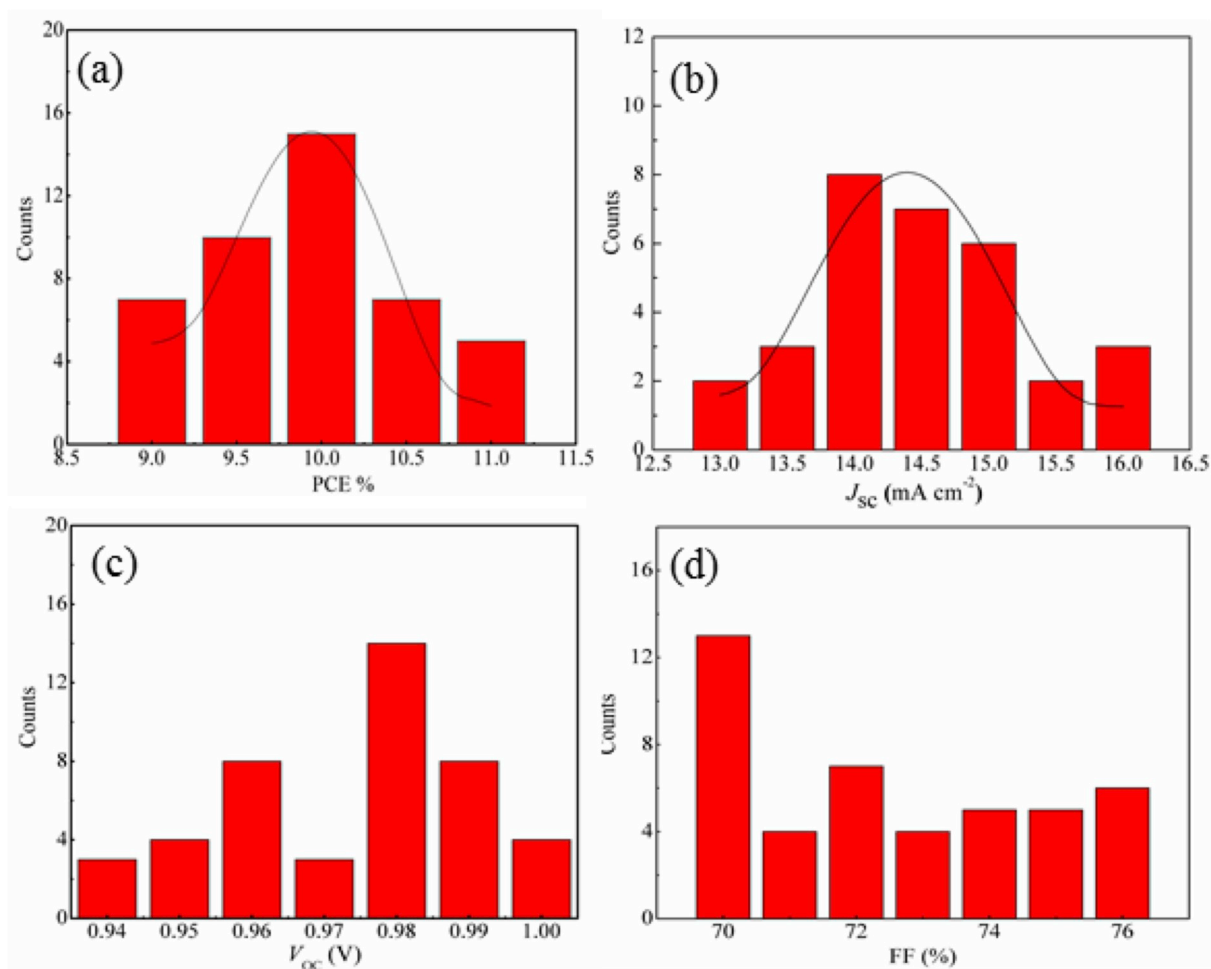


Fig. 4. Histograms of PCE, J_{sc} , V_{oc} , and FF for 44 devices.

Acknowledgements

This work was supported by the Shandong Provincial Natural Science Foundation, China (ZR2017ZB0314). X. Bao thanks the Youth Innovation Promotion Association CAS for financial support (2016194), and Aziz Saparbaev thanks the Chinese Academy of Sciences and the Third World Academy of Sciences (CAS-TWAS) for financial support.

Appendix A. Supplementary data

Supplementary data to this article can be found online at <https://doi.org/10.1016/j.jpowsour.2019.04.025>.

References

- [1] L. Meng, Y. Zhang, X. Wan, C. Li, X. Zhang, Y. Wang, X. Ke, Z. Xiao, L. Ding, R. Xia, H. Yip, Y. Cao, Y. Chen, *Science* 361 (2018) 1094–1098.
- [2] Y. Liu, J. Zhao, Z. Li, C. Mu, W. Ma, H. Hu, K. Jiang, H. Lin, H. Ade, H. Yan, *Nat. Commun.* 5 (2014) 5293.
- [3] J. Li, Z. Liang, Y. Wang, H. Li, J. Tong, X. Bao, Y. Xia, *J. Mater. Chem. C* 6 (2018) 11015–11022.
- [4] J. Li, Y. Wang, Z. Liang, N. Wang, J. Tong, C. Yang, X. Bao, Y. Xia, *ACS Appl. Mater. Interfaces* 11 (2019) 7022–7029.
- [5] N.J. Jeon, J.H. Noh, Y.C. Kim, W.S. Yang, S. Ryu, S.I. Seok, *Nat. Mater.* 13 (2014) 897–903.
- [6] X. Bao, Q. Zhu, M. Qiu, A. Yang, Y. Wang, D. Zhu, J. Wang, R. Yang, *J. Mater. Chem. A* 3 (2015) 19294–19298.
- [7] Q. Dong, Y. Fang, Y. Shao, P. Mulligan, J. Qiu, L. Cao, J. Huang, *Science* 347 (2015) 967–970.
- [8] J. Ding, S. Du, Y. Zhao, Z. Zuo, H. Cui, X. Zhan, Y. Gu, H. Sun, *J. Mater. Sci.* 52 (2017) 276–28.
- [9] W. Zhang, G.E. Eperon, H.J. Snaith, *Nat. Energy* 1 (2016) 16048.
- [10] J. Ding, S. Du, Z. Zuo, Y. Zhao, H. Cui, X. Zhan, *J. Phys. Chem. C* 121 (2017) 4917–4923.
- [11] A. Kojima, K. Teshima, K. Shirai, T.J. Miyasaka, *J. Am. Chem. Soc.* 131 (2009) 6050–6051.
- [12] NREL, Efficiency chart, <https://www.nrel.gov/pv/assets/images/efficiency-chart-20180716.jpg>.
- [13] W.S. Yang, B.K. Park, E.H. Jung, N.J. Jeon, Y.C. Kim, D.U. Lee, S.S. Shin, J. Seo, E.K. Kim, J.H. Noh, S.I. Seok, *Science* 356 (2017) 1376–1379.
- [14] W. Deng, X. Liang, P.S. Kubiak, P.J. Cameron, *Adv. Energy Mater.* 8 (2018) 1701544.
- [15] D. Bryant, N. Aristidou, S. Pont, M. Sanchez-Molina, T. Chotchanangachaval, S. Wheeler, J.R. Durrant, S.A. Haque, *Energy Environ. Sci.* 9 (2016) 1655–1660.
- [16] J.C. Ke, A. Walton, D.J. Lewis, A. Tedstone, P. O'Brien, A.G. Thomas, W.R. Flavell, *Chem. Commun.* 53 (2017) 5231–5234.
- [17] E.J. Juarez-Perez, Z. Hawash, S.R. Raga, L.K. Ono, Y. Qi, *Energy Environ. Sci.* 9 (2016) 3406–3410.
- [18] Y. Yuan, Q. Wang, Y. Shao, H. Lu, T. Li, A. Gruverman, J. Huang, *Adv. Energy Mater.* 6 (2016) 1501803.
- [19] E. Mosconi, A. Amat, M.K. Nazeeruddin, M. Grätzel, F.D. Angelis, *J. Phys. Chem. C* 117 (2013) 13902–13913.
- [20] E.M. Sanhira, A.R. Marshall, J.A. Christians, S.P. Harvey, P.N. Ciesielski, L.M. Wheeler, P. Schulz, L.Y. Lin, M.C. Beard, J.M. Luther, *Sci. Adv.* 3 (2017) eaao4204.
- [21] Y.G. Kim, T.Y. Kim, J.H. Oh, K. Soon Choi, Y.J. Kim, S.Y. Kim, *Phys. Chem. Chem. Phys.* 19 (2017) 6257–6263.
- [22] H. Choi, J. Jeong, H.-B. Kim, S. Kim, B. Walker, G.-H. Kim, J.Y. Kim, *Nano Energy* 7 (2014) 80–85.
- [23] M. Ahmad, G. Rehman, L. Ali, M. Shafiq, R. Iqbal, R. Ahmad, T. Khan, S. Jalali-Asadabadi, M. Maqbool, I. Ahmad, *J. Alloy. Comp.* 705 (2017) 828–839.
- [24] H. Choi, J. Jeong, H. Kim, S. Kim, B. Walker, G. Kim, J.Y. Kim, *Nano Energy* 7 (2014) 80–85.
- [25] G. Eperon, G. Paterno, R. Sutton, A. Zampetti, A. Haghighirad, F. Cacialli, H. Snaith, *J. Mater. Chem.* 3 (2015) 19688–19695.
- [26] P. Luo, W. Xia, S. Zhou, L. Sun, J. Cheng, C. Xu, Y. Lu, *J. Phys. Chem. Lett.* 7 (2016) 3603–3608.
- [27] D.Y. Heo, S.M. Han, N.S. Woo, Y.J. Kim, T. Kim, Z. Luo, S.Y. Kim, *J. Phys. Chem. C* 122 (2018) 15903–15910.

- [28] X. Ding, H. Chen, Y. Wu, S. Ma, S. Dai, S. Yang, J. Zhu, *J. Mater. Chem. A* 6 (2018) 18258–18266.
- [29] B. Li, Y. Zhang, L. Fu, T. Yu, S. Zhou, L. Zhang, L. Yin, *Nat. Commun.* 9 (2018) 1076.
- [30] S. Xiang, Z. Fu, W. Li, Y. Wei, J. Liu, H. Liu, L. n Zhu, R. Zhang, H. Chen, *ACS Energy Lett.* 3 (2018) 1824–1831.
- [31] Y. Wang, T. Zhang, M. Kan, Y. Zhao, *J. Am. Chem. Soc.* 140 (2018) 12345–12348.
- [32] P. Wang, X. Zhang, Y. Zhou, Q. Jiang, Q. Ye, Z. Chu, X. Li, X. Yang, Z. Yin, *J. You, Nat. Commun.* 9 (2018) 2225.
- [33] B. Zhao, S. Jin, S. Huang, N. Liu, J. Ma, D. Xue, Q. Han, J. Ding, Q. Ge, Y. Feng, J. Hu, *J. Am. Chem. Soc.* 140 (2018) 11716–11725.
- [34] C. Yang, J. Wang, X. Bao, J. Gao, Z. Liu, R. Yang, *Electrochim. Acta* 281 (2018) 9–16.
- [35] D.M. Trots, S.V. Myagkota, *J. Phys. Chem. Solids* 69 (2008) 2520–2526.
- [36] M. Liu, M. Johnston, H. Snaith, *Nature* 501 (2013) 395–398.
- [37] Z.G. Ji, S.C. Zhao, C. Wang, K. Liu, *Mater. Sci. Eng. B* 117 (2005) 63–66.
- [38] O.N. Yunakova, V.K. Miloslavskii, E.N. Kovalenko, *Optic Spectrosc.* 112 (2012) 91–96.
- [39] D. Zhang, S.W. Eaton, Y. Yu, L. Dou, P. Yang, *J. Am. Chem. Soc.* 137 (2015) 9230–9233.
- [40] X. Bao, Y. Wang, Q. Zhu, N. Wang, D. Zhu, J. Wang, A. Yang, R. Yang, *J. Power Sources* 297 (2015) 53–58.
- [41] J. Kruger, R. Plass, C. Le, M. Piccirelli, M. Gratzel, U. Bach, *Appl. Phys. Lett.* 79 (2001) 2085–2087.
- [42] G. Gao, H. Dong, X. Bao, Y. Zhang, A. Saparbaev, Yu, S. Wen, R. Yang, L. Dong, *J. Mater. Chem. C* 6 (2018) 8234–8241.
- [43] Y. Zhang, J. Wang, J. Xu, W. Chen, D. Zhu, W. Zheng, X. Bao, *RSC Adv.* 6 (2016) 79952–79957.
- [44] M. Uddin, T. Lee, S. Xu, S. Park, T. Kim, S. Song, T. Nguyen, S. Ko, S. Hwang, J. Kim, H. Woo, *Chem. Mater.* 27 (2015) 5997–6007.
- [45] X. Bao, Y. Zhang, J. Wang, D. Zhu, C. Yang, Y. Li, C. Yang, J. Xu, R. Yang, *Chem. Mater.* 29 (2017) 6766–6771.